Chapter-5

Holmium doped Lead Tungsten Tellurite glasses for Green Luminescence Applications

Paper based on this chapter is published in Journal of Luminescence, 163 (2015) 54-71

5.1. Introduction

Glassy materials doped with rare earth and transition metal ions have attracted a good amount of attention among the scientist because of their applications in visible and mid-infrared regions of the electromagnetic spectrum such as lasers, optical fibres, sensors, biomedical diagnostics, infrared detectors, marine optical communications, up-conversion lasers, optical data storage, atmospheric probing and high density memory storage devices [160-163]. Recently research work on tellurium based glasses increasing because of their promising technological applications in diversified fields [164-169]. Tellurium oxide (TeO_2) being a semiconductor in both crystalline and amorphous forms, with its superior physical and chemical properties, is aptly suitable for various technological devices such as ɤ-ray detectors, nonlinear optoelectronic devices and optical recording systems [170–174]. Considering the scientific patronages offered by PbF_2, WO_3 and TeO_2, we prepared Lead Tungsten Telluride (LTT) glasses using these chemicals as constituent elements to study the luminescence properties of these glasses doped with different rare earth ions. The encouraging results obtained for Pr^{3+} ions doped in LTT glasses for visible red lasers [175] prompted us to investigate Ho^{3+} ions in LTT glasses to know about their suitability for visible green luminescence. Among all the trivalent rare earth ions, Ho^{3+} ion is one of the most attractive ion for spectroscopic studies, because of several electronic transitions it can give in the visible and IR regions [176-178], which have relatively long-lived $^5I_7$ level and large peak stimulated emission cross-sections [179,180]. It has been confirmed that mid infrared laser emission of Ho^{3+} ion is in the range of 1.2 - 4.9 μm [181,182]. The mid infrared emission of Ho^{3+} ion gives eye-safe laser emission at room temperature (RT) with a relatively low threshold action that has smart applications in the devices such as LIDAR and in atmospheric communication systems [183]. Moreover, the $^5F_4 \rightarrow {}^5I_8$ transition of Ho^{3+} ion is a hypersensitive transition and hence host dependent one. For this reason glasses doped with Ho^{3+} ions are the most important candidates for both visible (~547 nm) ($^5F_4 \rightarrow {}^5I_8$) and mid infrared (~2 μm) ($^5I_7 \rightarrow {}^5I_8$) regions and are useful for the development of solid state lasers in visible and mid infrared regions.

In the present work, LTT glasses doped with Ho^{3+} ions at different concentrations were prepared to study the absorption and photoluminescence spectral properties to understand the suitability of these materials for visible luminescence. From the absorption and emission spectral measurements, different radiative properties

such as transition probability, radiative lifetimes, branching ratios and emission cross-sections were estimated for the observed emission transitions of Ho^{3+} ions. The CIE colour co-ordinates are also evaluated from the measured emission spectra to understand the utility of these glasses for green light emission.

5.2. Experimental

5.2.1. Synthesis of LTT Glasses

LTT glasses doped with different concentrations of Ho^{3+} ions with chemical composition of $15PbF_2$ - $25WO_3$ - (60-x) TeO_2 – xHo_2O_3 (x=0.1, 0.5, 1.0, 1.5, 2.0 and 2.5 mol %) were prepared by using melt quenching method as described in Chapter-II. The samples used in the present work are referred according to the doping concentration of Ho_2O_3 as LTTHo01, LTTHo05, LTTHo10, LTTHo15, LTTHo20 and LTTHo25 glasses. In order to measure the optical spectra, the glasses were polished (0.2 cm thickness) for optical quality.

5.2.2. Physical and Optical Measurements

The densities of Ho^{3+} ions doped LTT glasses were measured by using Archimedes's principle with water as an immersion liquid. The refractive indices of the prepared glasses were measured using Brewster's angle method with He-Ne laser operating at 632 nm. Using refractive indices and densities, some other physical properties were also measured using suitable equations (2.1-2.11) which are given in chapter-2 and are presented in Table 5.1. In the present study the physical properties are changing from glass to glass with increase in the concentration of Ho^{3+} ions, indicating the change in environment around the doped Ho^{3+} ions. The optical absorption spectra were measured for all the glass samples from 400 to 2200 nm at room temperature with a specified resolution 0.1 nm using a Jasco V-670 UV-vis-NIR spectrometer. Schimadzu RF-5301 PC Spectrofluorophotometer was used to record the photoluminescence excitation and emission spectra for all these glasses at room temperature.

5.3. Results and Discussion

5.3.1 Physical Properties

The physical properties of glassy materials play a vital role in prediction of optical properties. Density and refractive index of glass samples play an important role in evaluating the other physical properties such as Average molecular, weight mean

atomic volume etc. All such physical properties evaluated for the present LTT glasses are given in Table 5.1. Fig. 5.1(a), shows the variation of density and refractive indices of the titled glasses with Ho^{3+} concentration.

Table 5.1.

Various physical properties of Ho^{3+} ions in LTT glasses

Physical Property	**LTTHo01**	**LTTHo05**	**LTTHo10**	**LTTHo15**	**LTTHo20**	**LTTHo25**
Refractive index (n_d)	2.400	2.404	2.407	2.415	2.435	2.437
Density, d (gm/cm^3)	6.608	6.618	6.631	6.643	6.656	6.668
Average molecular weight, $\bar{M}$(g)	190.7	191.5	192.6	193.7	194.8	195.9
Ho^{3+} ion concentration, N (10^{22} ions/cm^3)	0.208	1.040	2.072	3.096	4.113	5.123
Mean atomic volume (g/cm^3/atom)	8.875	8.880	8.886	8.893	8.898	8.905
Optical dielectric constant ($p\,\partial t/\partial p$)	4.763	4.783	4.793	4.835	4.932	4.938
Dielectric constant (ϵ)	5.733	5.783	5.793	5.835	5.932	5.938
Reflection losses (R %)	0.169	0.170	0.170	0.171	0.174	0.174
Molar refraction (R_m)(cm^{-3})	17.70	17.79	17.87	18.00	18.20	18.28
Polaron radius (r_p) (Å)	5.013	2.935	2.332	2.040	1.856	1.725
Inter-atomic distance (r_i) (Å)	7.838	4.588	3.646	3.189	2.901	2.697
Molecular electronic polarizability, α (10^{-23}cm^3)	7.023	1.411	0.708	0.475	0.361	0.290
Field strength ,F (10^{15}cm^{-2})	1.193	3.483	5.513	7.205	8.707	10.07
Optical basicity ,(Λ_{th})	0.464	0.467	0.470	0.474	0.478	0.482

From Fig. 5.1(a) it can be observed that the density and refractive indices of titled glasses moderately increases with the increase of Ho^{3+} ion concentration. Increase in number of bridging oxygen ions will increase the compactness of the glass and there by increases the density of the glasses used in the present work. Consequently this leads to increase in the rigidity of the prepared glasses.

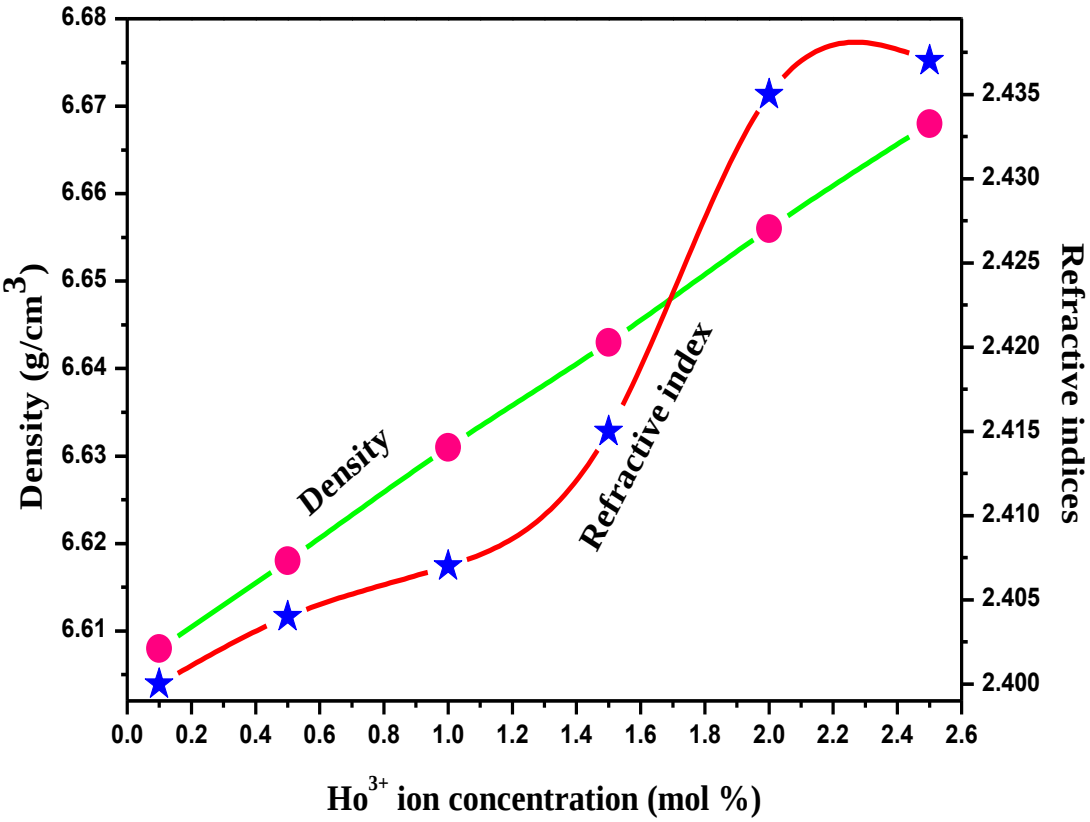

Fig. 5.1(a). Variation of density and refractive index with Ho^{3+} ion concentration in LTT Glasses

Fig. 5.1(b) shows the variation of inter atomic distance and average molecular weight with Ho^{3+} ion concentration in titled glasses. From Fig. 5.1(b) it can be observed that the average molecular weight increases whereas inter atomic distance decreases with the increasing of Ho^{3+} ion concentration. This indicates that the atoms present in the titled glass network are more tightly packed.

5.3.2. Absorption Spectral Analysis

Fig. 5.2 represents the absorption spectrum of Ho^{3+} ions doped LTTHo10 glass. The spectrum exhibits nine absorption bands in the vis-NIR regions centred at 452, 469, 476, 489, 538, 643, 890, 1153 and 1956 nm corresponding to the transitions $^5I_8 \rightarrow {}^5G_6$, $^5I_8 \rightarrow {}^3K_8$, $^5I_8 \rightarrow {}^5F_2$, $^5I_8 \rightarrow {}^5F_3$, $^5I_8 \rightarrow {}^5F_4$, $^5I_8 \rightarrow {}^5F_5$, $^5I_8 \rightarrow {}^5I_5$, $^5I_8 \rightarrow {}^5I_6$ and $^5I_8 \rightarrow {}^5I_7$ respectively. The absorption spectrum shown in Fig. 5.2 is in consistent with the spectra reported for Ho^{3+} ions doped oxyfluoride [184], fluoride [185], tellurite [186] and fluoronidate [187] glasses.

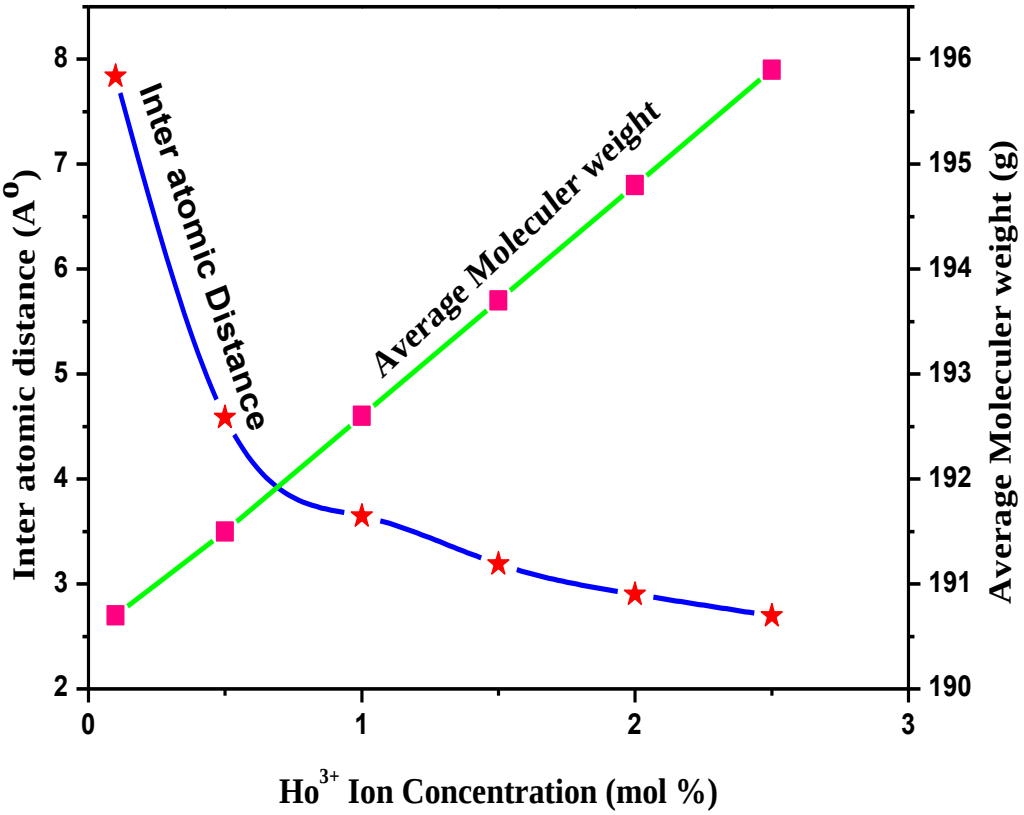

Fig. 5.1(b). Variation of inter atomic distance and average molecular weight with Ho^{3+} ion concentration in LTT Glasses

The absorption bands observed in the visible and NIR regions are attributed to the 4*f*–4*f* transitions of Ho^{3+} ions from the $^5I_8$ ground state to various excited states as presented in Table 5.3. The identification and assignment of energy levels are in accordance with Carnall et.al [105]. From Fig. 5.2 it is observed that the absorption bands $^5I_8 \rightarrow {}^5G_6$ (452 nm), $^5I_8 \rightarrow {}^5F_4$ (538 nm), $^5I_8 \rightarrow {}^5F_5$ (643 nm) are relatively more intense and sharp than the other transitions. The bands corresponding the transitions $^5I_8 \rightarrow {}^3K_8$ (469 nm), $^5I_8 \rightarrow {}^5F_2$ (476 nm), $^5I_8 \rightarrow {}^5F_3$ (489 nm) are found to be very weak while the bands due to $^5I_8 \rightarrow {}^5I_5$ (890 nm), $^5I_8 \rightarrow {}^5I_6$ (1153 nm) and $^5I_8 \rightarrow {}^5I_7$ (1956 nm) transitions are broad and weak. In general, the absorption transitions of rare earth ions are induced electric dipole in nature and magnetic dipole contribution is insignificant. However in case of

Ho^{3+} ion, the transition $^5I_8 \rightarrow {}^5I_7$ (1956 nm) contains some magnetic dipole contribution [186].

The pattern of absorption spectra for all the six Ho^{3+} ions doped LTT glasses remains the same and the intensity of the bands have been perceived. From these energy bands, the nephelauxetic ratio and bonding parameters have been evaluated using eq.(1.3,1.4) to get an idea about the nature of Ho^{3+} ligand bond in the present work and are given in Table 5.2.

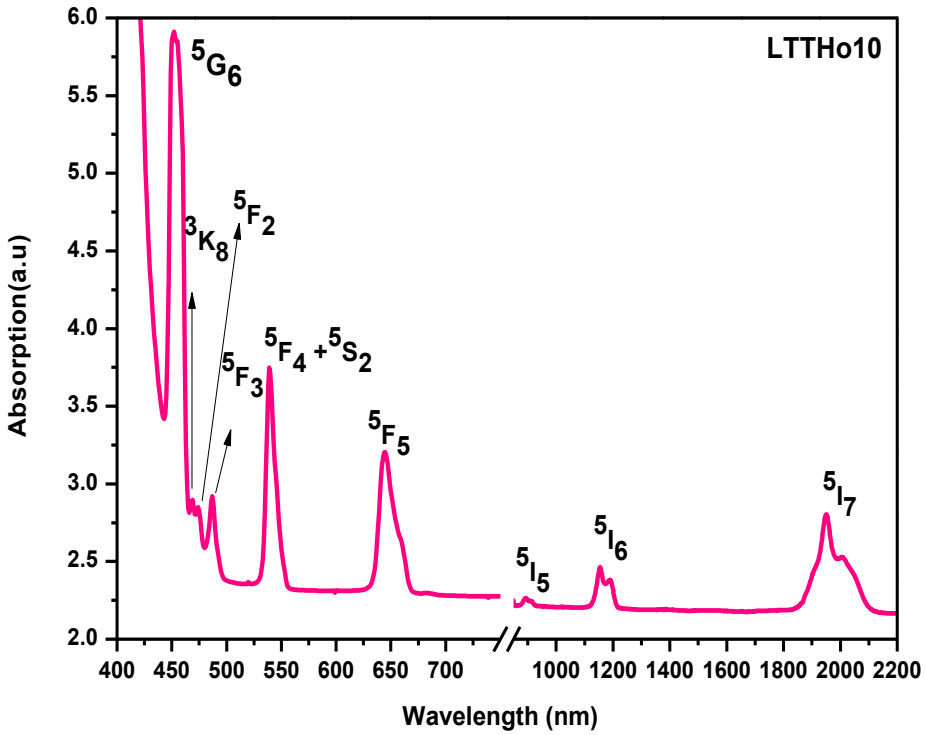

Fig. 5.2. Optical absorption spectrum of the LTTHo10 glass

The nephelauxetic ratio (β) is calculated by using the eq. (1.3) given in chapter-I.

From the average values of $\bar{\beta}$ the bonding parameter δ is calculated using eq.(1.4) given in chapter-I.

Table 5.2.

Observed band positions (cm^{-1}) and bonding parameters ($\bar{\beta}$ and δ) of Ho^{3+} ions in LTT glasses

Transition	LTTHo01	LTTHo05	LTTHo10	LTTHo15	LTTHo20	LTTHo25
$^5I_7$	5128	5134	5131	5128	5138	5131
$^5I_6$	8673	8674	8678	8677	8669	8669
$^5I_5$	11187	11058	11213	11193	11203	11223
$^5F_5$	15527	15513	15505	15501	15520	15531
$^5F_4$	18552	18564	18548	18543	18561	18554
$^5F_3$	20533	20567	20534	20563	20562	20519
$^5F_2$	--	21091	21093	21100	21090	21079
$^3K_8$	--	21349	21316	21312	21364	21321
$^5G_6$	22026	22187	22097	22187	22187	22105
$\bar{\beta}$	0.9991	0.9987	0.9985	0.9984	0.9981	0.9979
δ	0.088	0.120	0.140	0.150	0.180	0.200

Depending on the field of environment, the bonding parameter may be positive or negative indicating covalent or ionic bonding. In the present work, the positive values obtained for the bonding parameter $'\delta'$ indicates the bonding nature between Ho-O bond is covalent in nature.

From the measured absorption spectra of Ho^{3+} ions doped LTT glasses, the experimental oscillator strengths were measured using areas under the absorption peaks by using eq.(1.8) given in chapter-I. The oscillator strengths of absorption bands are calculated using J-O theory with the predictable equations [47, 48].

The quality of the fit is measured by root mean square deviation (δ_{rms}) between the calculated and experimental oscillator strengths by using the following equation and the measured values of f_{exp} and f_{cal} together with the r.m.s deviation are represented in Table 5.3. The deviation parameter δ_{rms} is calculated by using the expression given in literature [188,189]. From Table 5.3, it is observed that, the oscillator strengths vary from glass to glass and these variations are very small.

The J-O intensity parameters Ω_2, Ω_4 and Ω_6 are evaluated through least square fitting analysis given in literature [136], for the present glasses are given in Table 5.4 along with the other reported values. Few transitions of rare earths are found to be very sensitive to the doped rare earth ion concentration and glass composition. These absorption levels show unusual intensity variations and are called as hypersensitive levels. For the Ho^{3+} ion, the transition $^5I_8 \rightarrow {}^5G_6$ is hypersensitive transitions which satisfies the selection rules such as $|\Delta S| = 0$, $|\Delta L| \leq 2$, $|\Delta J| \leq 2$ .The spectral oscillator strengths of these transitions are strongly observed by the Judd-Ofelt (Ω_2) parameter [190, 191].

From Table 5.3 [192-199], it is observed that the hypersensitive level ($^5G_6$) is appeared as more intense than other bands and significant variations were exhibited by them due to the changes in the Judd-Ofelt (Ω_2) parameter for all the glasses. In the present investigation, in all the glasses under investigation, the J-O parameters follow the trend $\Omega_4 > \Omega_2 > \Omega_6$. Among all the glasses, LTTHo10 glass possesses maximum values of J-O intensity parameters than other LTT glasses and other reported values [192-199]. The J-O intensity parameters magnitude is mainly related with the physical and chemical properties such as viscosity and covalent character of the chemical bonds. The large values of Ω_2 J-O parameter indicate the covalent nature of the chemical bonds between the glass matrix and rare earth ions. The asymmetry of the sites in the neighbourhood of rare earth ion also depends upon this Ω_2 parameter.

Table 5.3.

Experimental (f_{exp} x 10^{-6}) and calculated (f_{cal} x 10^{-6}) oscillator strengths and rms deviation of Ho^{3+} ions in LTT glasses

Transitions from 5I8→	**LTTHo01**		**LTTHo05**		**LTTHo10**		**LTTHo15**		**LTTHo20**		**LTTHo25**	
	f_{exp}	**f_{cal}**	**f_{exp}**	**f_{cal}**	**f_{exp}**	**f_{cal}**	**f_{exp}**	**f_{cal}**	**f_{exp}**	**F_{cal}**	**f_{exp}**	**f_{cal}**
5G6	30.1	30.1	45.0	44.9	69.7	69.6	60.2	60.1	56.4	56.3	52.6	52.5
$^3K_8$	--	9.40	0.20	5.51	0.31	9.01	0.27	7.22	0.23	3.06	0.23	5.05
$^5F_2$	--	4.40	0.57	1.65	1.01	2.73	0.88	2.16	0.99	2.19	0.75	1.43
$^5F_3$	2.57	1.96	1.74	2.89	2.79	4.80	2.27	3.79	2.67	3.85	1.75	2.51
$^5F_4$	6.02	4.44	8.30	5.62	14.6	8.98	12.0	7.23	10.7	7.16	9.52	5.29
$^5F_5$	8.27	8.54	8.96	9.81	13.8	15.2	11.2	12.4	11.3	12.1	8.68	9.75
$^5I_5$	0.63	0.39	0.99	0.53	0.71	0.86	0.57	0.69	0.51	0.69	0.41	0.48
$^5I_6$	1.86	1.99	2.13	2.82	4.91	4.62	4.06	3.68	2.95	3.70	1.91	2.53
$^5I_7$	2.73	2.84	4.51	3.92	6.92	6.41	5.46	5.12	5.31	5.13	3.98	3.58
δ_{rms}(x10-6)	±0.649		±2.098		±3.604		±2.932		±1.65		±2.207	

If the Ω_2 parameter value is high then the degree of asymmetry around the rare earth ion will be high. Not only this, the covalency of rare earth ion-oxygen bond also becomes stronger. In the present series of glasses, LTTHo10 glass possesses maximum value of Ω_2 parameter. Therefore LTT glass with 1 mol% of Ho^{3+} ions possesses higher asymmetry and greater degree of covalency of holmium ion and oxygen bond than other reported values [192-199]. The large values of Ω_4 and Ω_6 are related to the bulk properties such as viscosity and rigidity of the glass structure.

Table 5.4.

Judd-Ofelt Parameters (Ω_λ x $10^{-20}cm^2$) of the Ho^{3+} ions in LTT glasses.

Glass System	Ω_2	Ω_4	Ω_6	Trend	References
LTTHo01	2.00	5.21	1.54	$\Omega_4>\Omega_2>\Omega_6$	present work
LTTHo05	4.33	5.28	2.27	$\Omega_4>\Omega_2>\Omega_6$	present work
LTTHo10	6.66	7.71	3.68	$\Omega_4>\Omega_2>\Omega_6$	present work
LTTHo15	6.01	6.52	2.96	$\Omega_4>\Omega_2>\Omega_6$	present work
LTTHo20	5.47	6.08	2.95	$\Omega_4>\Omega_2>\Omega_6$	present work
LTTHo25	5.41	5.62	1.97	$\Omega_4>\Omega_2>\Omega_6$	present work
ZrF_2-BaF_2	2.12	2.38	1.61	$\Omega_4>\Omega_2>\Omega_6$	[192]
ZBLAN	1.90	2.09	1.56	$\Omega_4>\Omega_2>\Omega_6$	[193]
$YAlO_3$	1.82	2.38	1.53	$\Omega_4>\Omega_2>\Omega_6$	[194]
MHGHo	2.07	2.38	1.53	$\Omega_4>\Omega_2>\Omega_6$	[195]
La2O3	6.52	2.22	2.53	$\Omega_2>\Omega_6>\Omega_2$	[196]
PbO-ZnO-B2O3	2.77	2.26	1.50	$\Omega_2>\Omega_4>\Omega_6$	[197]
Fluoride	2.40	1.70	1.80	$\Omega_2>\Omega_6>\Omega_4$	[198]
HBLACs	1.53	3.19	4.93	$\Omega_6>\Omega_4>\Omega_2$	[199]

5.3.3. Analysis of Emission spectra and Estimation of Radiative properties

It is well known that rare earth ions doped materials exhibit sharp excitation and emission bands. In order to know the excitation wavelength to record the emission spectra, we have recorded the excitation spectra for the LTTHo10 glasses by fixing the emission wavelength at 545 nm. Fig. 5.3 shows the excitation spectrum of 1 mol % of Ho^{3+} ions doped LTT glass (LTTNd10) in the wavelength range 325 to 500 nm. As shown in Fig. 5.3, the excitation spectra consists of five excitation bands centred at 349 nm, 419 nm, 452 nm, 473 nm, and 486 nm corresponding to the transitions $^5I_8\rightarrow{}^5G_3$, $^5I_8\rightarrow(^5G+{}^3G)_5$, $^5I_8\rightarrow{}^5G_6$, $^5I_8\rightarrow{}^3K_8$ and $^5I_8\rightarrow{}^5F_3$ respectively. Among the five excitation bands observe, a band centred at 452 nm is relatively more intense than the others.

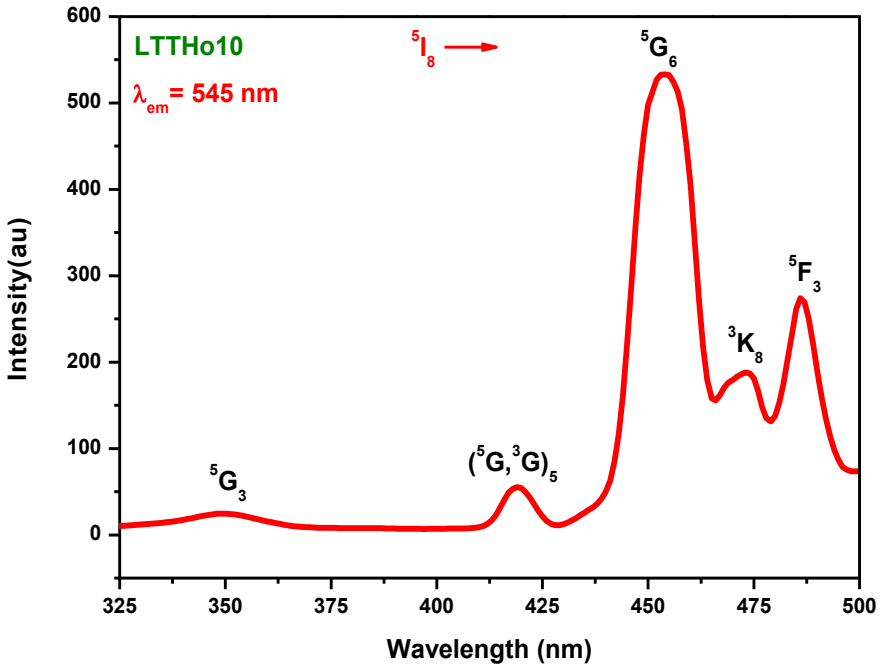

Fig. 5.3. Excitation spectrum of the LTTHo10 glass

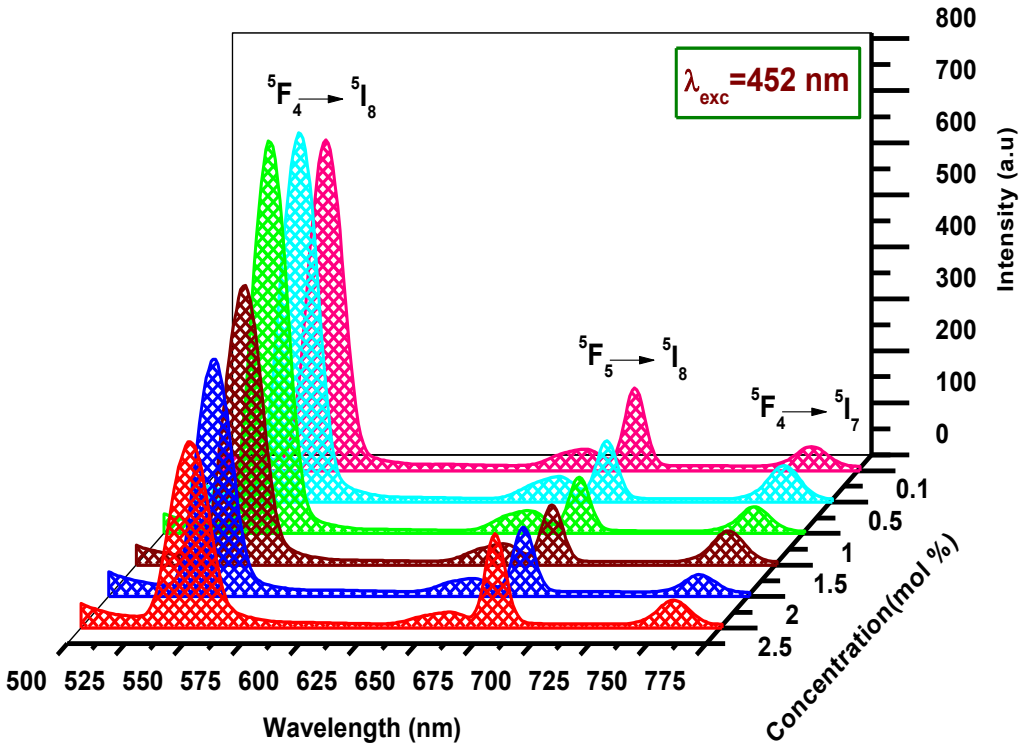

Fig. 5.4. Emission spectra of Ho^{3+} ions in LTT glasses

By using this intense excitation wavelength, the emission spectra for all the Ho^{3+} ions doped LTT glasses were recorded to investigate the luminescence characteristics.

Fig. 5.4 shows the emission spectra of Ho^{3+} ions in LTT glasses in the wavelength range 500 to 775 nm at an excitation wavelength 452 nm. The emission spectra show three bands corresponding to the transitions $^5F_4 \rightarrow {}^5I_8$ (546 nm), $^5F_5 \rightarrow {}^5I_8$ (679 nm) and $^5F_4 \rightarrow {}^5I_7$ (755 nm). Among the three emission transitions, a band corresponding to the transition $^5F_4 \rightarrow {}^5I_8$ is relatively more intense than the other bands and falls in the visible green region (546 nm). When the Ho^{3+} ions are excited to $^5F_4$ and $^5I_6$ levels radiative and non-radiative (NR) relaxations take place due to the closely spaced higher energy levels. From Fig. 5.4, it is clearly observed that the intensity of $^5F_4 \rightarrow {}^5I_8$ transition is higher than that of the $^5F_5 \rightarrow {}^5I_8$ transition. From Fig. 5.4, it is also observed that the intensity of $^5F_4 \rightarrow {}^5I_8$ transition increases from 0.1 to 1.0 mol% of Ho^{3+} ion concentration and then decreases beyond showing concentration quenching. This concentration quenching observed beyond 1 mol% of Ho^{3+} ion concentration may be due to resonance energy transfer between Ho ions at higher concentrations. Fig. 5.5 shows the energy level diagram which describes the absorption, excitation, emission (visible & NIR) and resonant energy transfer mechanisms of LTTHo10 glass. From Fig. 5.6, it is observed that, the overlap of absorption ($^5I_8 \rightarrow {}^5F_4$) and emission ($^5F_4 \rightarrow {}^5I_8$) bands in the spectral region 520–570 nm indicates the resonant energy transfer (RET) process among the Ho^{3+} ions.

To estimate the emission performance of Ho^{3+} doped LTT glasses, the radiative parameters such as spontaneous transition probabilities (A_R), total transition probabilities (A_T), radiative lifetimes (τ_R) and luminescence branching ratios (β_R) for all the emission transitions were evaluated by using the J-O parameters and are given in Table 5.5. All these radiative properties are evaluated by using the relevant equations (1.10-1.13) given in chapter-I. From Table 5.5 it is observed that, the LTTHo10 glass possesses maximum values for radiative transition properties. Generally the branching ratio (β_R) is a very important parameter to the laser designer, because it describes the possibility of getting stimulated emission from any particular transition. The fluorescence branching ratio which characterizes and makes the transition as potential for laser emission, if its value $\beta_R \geq 0.5$. As shown in Table 5.5, in present study the radiative and experimental branching ratios ($\beta_R = 0.505$ & $\beta_{exp} = 0.804$) for $^5F_4 \rightarrow {}^5I_8$

emission transition are found to be maximum for LTTHo10 glass than the other LTT glasses indicating the potentiality of this glass to produce visible green luminescence.

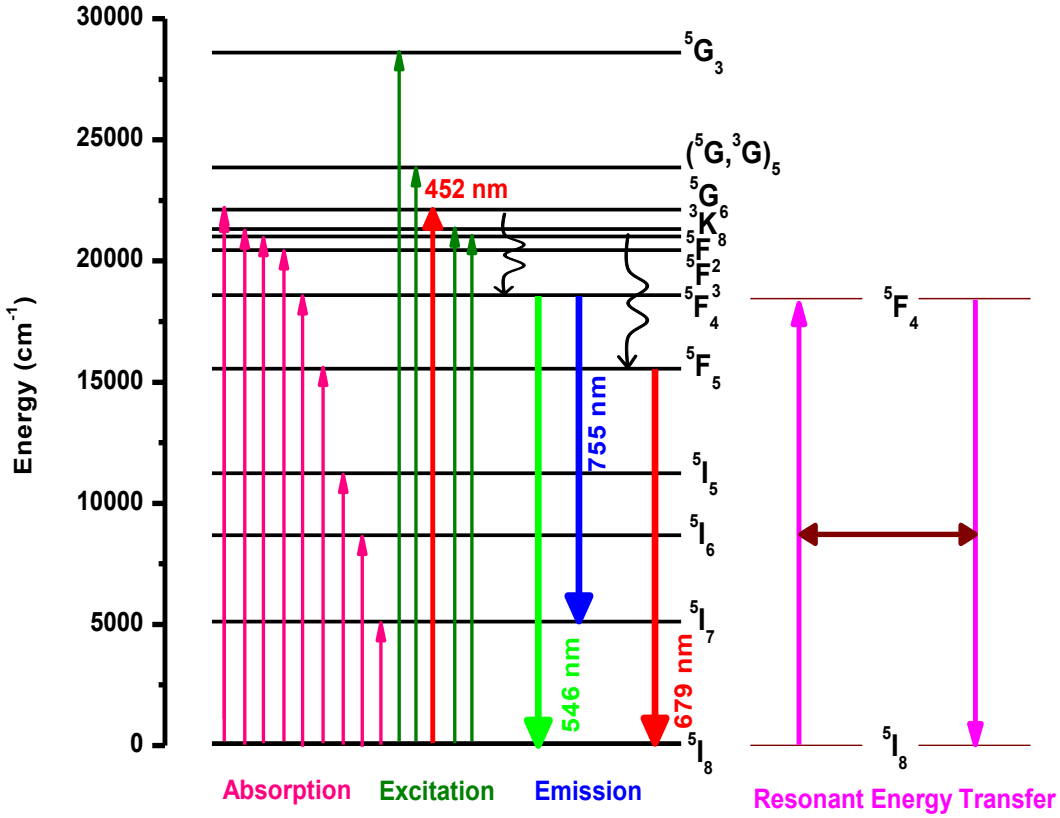

Fig. 5.5. Energy level scheme depicting the absorption, excitation, emission and resonant energy transfer mechanism of LTTHo10 glass

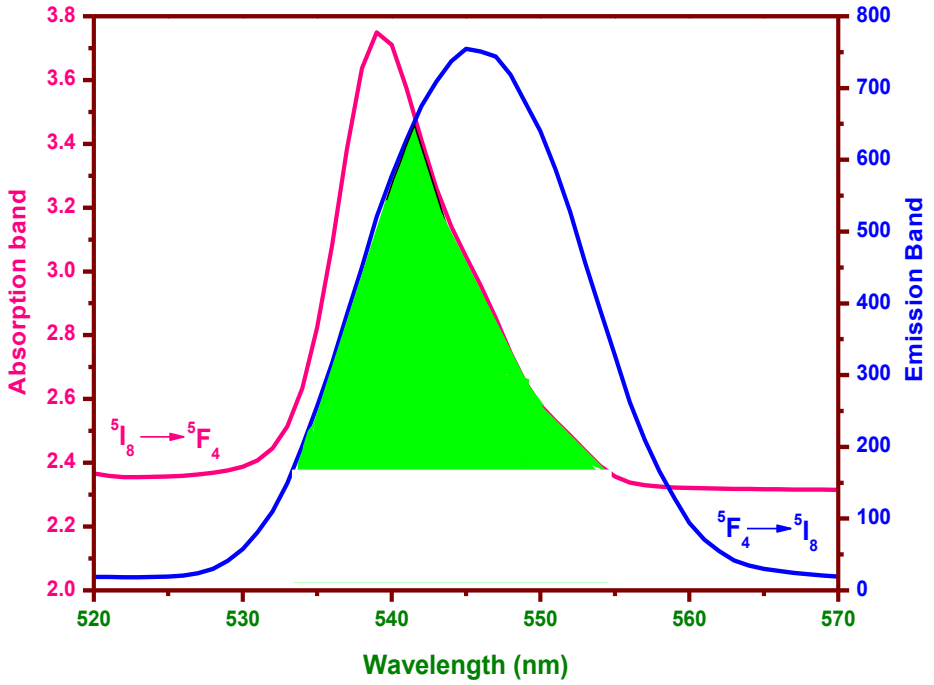

Fig. 5.6. The overlap of absorption and emission spectra of Ho^{3+} ions in LTT glass in the spectral region from 520 to 570 nm

Table 5.5.

Transition probabilities (A_R) (s^{-1}), luminescence branching ratios (β_R), total transition probability (A_T) (s^{-1}) and radiative lifetimes (τ_R) (μs) for the observed emission transitions of Ho^{3+} ions in LTT glasses

Transition	A_R	β_R	A_T	τ_R
LTTHo01				
$^5F_4 \rightarrow {}^5I_8$	1848.14	0.498	3705.86	269
$^5F_5 \rightarrow {}^5I_8$	795.55	0.499	1593.72	627
$^5F_4 \rightarrow {}^5I_7$	1493.21	0.402	3705.86	269
LTTHo05				
$^5F_4 \rightarrow {}^5I_8$	2743.18	0.504	5436.70	183
$^5F_5 \rightarrow {}^5I_8$	1180.83	0.505	2338.67	427
$^5F_4 \rightarrow {}^5I_7$	2216.36	0.407	5436.70	183
LTTHo10				
$^5F_4 \rightarrow {}^5I_8$	4462.55	0.505	8821.52	133
$^5F_5 \rightarrow {}^5I_8$	1920.95	0.506	3793.72	263
$^5F_4 \rightarrow {}^5I_7$	3605,53	0.408	8821.52	133
LTTHo15				
$^5F_4 \rightarrow {}^5I_8$	3640.70	0.505	7205.63	138
$^5F_5 \rightarrow {}^5I_8$	1567.18	0.505	3098.80	322
$^5F_4 \rightarrow {}^5I_7$	2941.52	0.408	7205.63	138
LTTHo20				
$^5F_4 \rightarrow {}^5I_8$	3750.23	0.506	7412.85	140
$^5F_5 \rightarrow {}^5I_8$	1614.32	0.508	3009.04	335
$^5F_4 \rightarrow {}^5I_7$	2845.13	0.410	7412.85	140
LTTHo25				
$^5F_4 \rightarrow {}^5I_8$	2509.73	0.501	5003.39	199
$^5F_5 \rightarrow {}^5I_8$	1180.83	0.505	2048.13	464
$^5F_4 \rightarrow {}^5I_7$	2216.36	0.405	5003.39	199

The stimulated emission cross-section (σ_{se}) is an another significant parameter which gives the rate of energy extraction from an optical material. From the observed emission bands, the stimulated emission cross-sections (σ_{se}) are calculated using eq.(1.14) is given in chapter-I and are presented in Table 5.6.

The large value of stimulated emission cross-section (σ_{se}) is a striking characteristic for low-threshold and high gain applications to get continuous wave laser action and it is also used to recognize the potential laser transitions of rare earth ions in any host matrix. From Table 5.6 it is seen that, all the transitions of LTTHo10 glass have lowest values of effective band width ($\Delta\lambda_p$). The main reason to get the lowest values of effective band width is the splitting of the transition levels and inhomogeneous broadening. The decrease in effective band width values are also an indication of weak asymmetry of the ligand field. Among all the glasses, the LTTHo10 glass possess highest stimulated emission cross-section (σ_{se}) for the transition $^5F_4 \rightarrow {}^5I_8$ (546 nm). Hence LTTHo10 glass is the most suitable one to produce visible green luminescence among all the LTT glasses studied in the present investigation. There are another two important parameters namely gain band width ($\sigma_{se} \times \Delta\lambda_P$) and optical gain ($\sigma_{se} \times \tau_R$) parameter, which are used to calculate the amplification of the host in which the rare earth ions are located. For a good optical amplifier, stimulated emission cross-section (σ_{se}), gain band width ($\sigma_{se} \times \Delta\lambda_P$) and optical gain ($\sigma_{se} \times \tau_R$) parameter values should be high. From Table 5.6, it is observed that, the glass LTTHo10 has higher values of stimulated emission cross-section (σ_{se}), gain band width ($\sigma_{se} \times \Delta\lambda_P$) and optical gain ($\sigma_{se} \times \tau_R$). Hence LTT glass doped with 1 mol% of Ho^{3+} ions is quite suitable for visible green luminescence applications and optical amplification.

Table 5.6.

Emission peak wavelength (λ_P)(nm), effective band widths ($\Delta\lambda_P$)(nm), radiative and experimental branching ratios (β_R & β_{exp}), stimulated emission cross-sections (σ_{se}) (x 10^{-21}) (cm^2), gain band width (σ_{se} x $\Delta\lambda_p$) (x 10^{-28}) (cm^3) and optical gain (σ_{se} x τ_R) (x 10^{-25}) (cm^2 s) parameters for the emission transitions of Ho^{3+} ions in LTT glasses.

Spectral parameters	**LTTHo01**	**LTTHo05**	**LTTHo10**	**LTTHo15**	**LTTHo20**	**LTTHo25**
			$^5F_4 \rightarrow {}^5I_8$ (Green)			
λ_P	546	546	546	546	546	546
$\Delta\lambda_p$	13.8	11.3	8.75	10.0	11.3	11.9
β_R	0.498	0.504	0.505	0.505	0.506	0.501
β_{exp}	0.749	0.777	0.804	0.739	0.719	0.658
σ_{se}	2.75	4.97	10.4	7.36	6.63	6.27
σ_{se} x $\Delta\lambda_p$	37.8	55.9	90.8	77.6	74.50	74.5
σ_{se} x τ_R	7.40	9.10	13.8	10.7	9.28	11.7
			$^5F_5 \rightarrow {}^5I_8$ (Red)			
λ_P	678	678	678	678	678	678
$\Delta\lambda_p$	13.8	13.8	12.5	15.0	15.6	16.3
β_R	0.499	0.505	0.506	0.505	0.508	0.505
β_{exp}	0.186	0.138	0.145	0.167	0.203	0.245
σ_{se}	2.81	4.16	7.44	5.02	4.88	3.14
σ_{se} x $\Delta\lambda_p$	38.7	57.2	93.0	75.3	76.3	51.0
σ_{se} x τ_R	17.60	17.80	19.60	16.20	16.30	14.60
			$^5F_4 \rightarrow {}^5I_7$ (Infrared)			
λ_P	755	755	755	755	755	755
$\Delta\lambda_p$	26.3	25.0	24.4	25.0	26.3	27.5
β_R	0.402	0.407	0.408	0.408	0.410	0.405
β_{exp}	0.064	0.056	0.076	0.092	0.076	0.096
σ_{se}	0.42	0.63	0.89	0.79	0.78	0.59
σ_{se} x $\Delta\lambda_p$	11.2	16.5	26.8	21.7	20.7	14.7
σ_{se} x τ_R	11.4	12.1	14.6	12.0	11.0	10.7

5.3.4 Evaluation of CIE colour co-ordinates:

The colour chromaticity coordinates for the LTT glasses doped with different concentrations of Ho^{3+} ions were evaluated from the luminescence spectra using the CIE (Commission International de l'Eclairage France) system. Fig. 5.7 presents the CIE plot with colour coordinates of the LTTHo10 glass calculated from the luminescence spectra recorded at an excitation wavelength at 452 nm. The chromaticity coordinates for the present glasses were calculated using eq.(1.21-1.25), [64-67] given in chapter-1 and the calculated values are presented in Table 5.7. The CIE colour coordinates evaluated for the Ho^{3+} doped LTT glasses are lying in the bright green region corresponding to $^5F_4 \rightarrow {}^5I_8$ transition at 546 nm emission wavelengths.

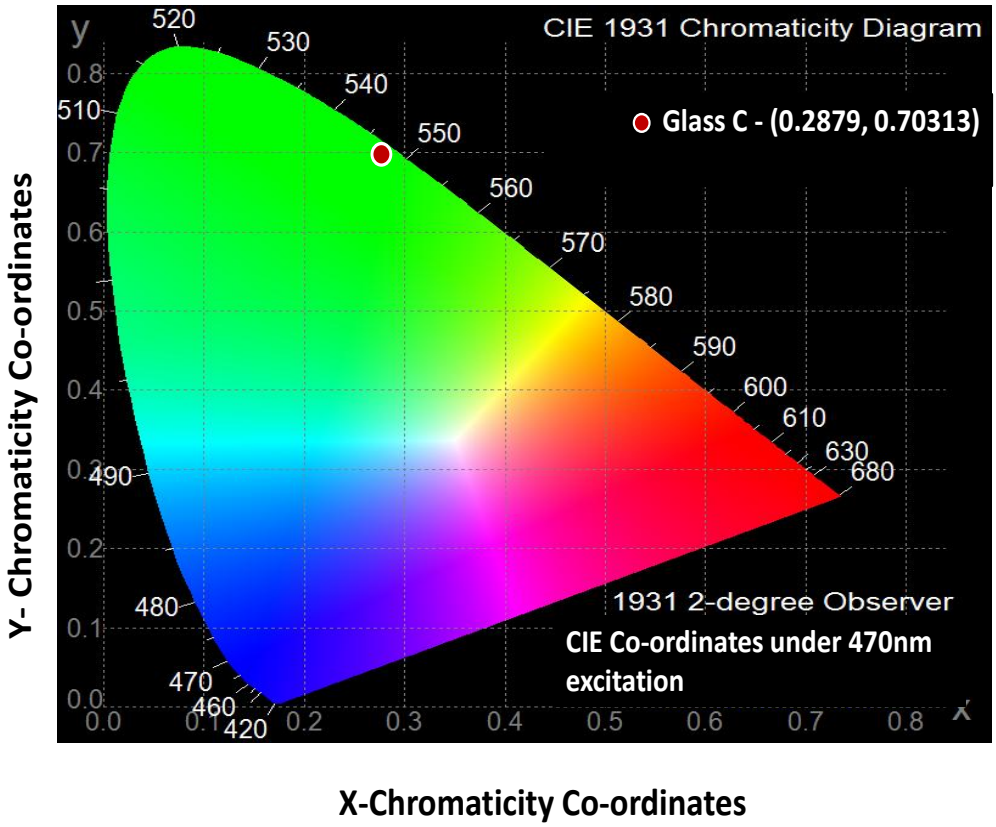

Fig. 5.7. CIE 1931chromaticity diagram for LTTHo10 glass

Table 5.7.

Colour co-ordinates of Ho^{3+} ions in LTT glasses at λ_{exc} = 452 nm wavelength.

Name of the Sample	Colour Co-ordinates
	λ_{exc} =452 nm
LTTHo01	(0.3082, 0.6819)
LTTHo05	(0.2879, 0.7031)
LTTHo10	(0.2858, 0.7069)
LTTHo15	(0.2844, 0.7070)
LTTHo20	(0.2780, 0.7126)
LTTHo25	(03022, 0.6911)

5.4. Conclusions

Lead Tungstun Tellurite glasses doped with different concentrations of Ho^{3+} ions were investigated using spectroscopic techniques such as absorption, excitation and emission to characterize and optimize the doped rare earth ions for visible emission. The photoluminescence spectra recorded for LTT glasses give three emission bands in green, red and NIR regions at 546, 679 and 755 nm corresponding to the transitions $^5F_4 \rightarrow {}^5I_8$, $^5F_5 \rightarrow {}^5I_8$ and $^5F_4 \rightarrow {}^5I_7$ respectively. The luminescence quenching observed for $^5F_4 \rightarrow {}^5I_8$ emission transition at 1 mol % of Ho^{3+} ion concentration is attributed to the resonance energy transfer among the excited Ho^{3+} ions. The branching ratio, stimulated emission cross-section values are found to be maximum for LTTHo10 glass than other LTT glasses. From all these studies, it is concluded that LTTHo10 glass can act as an efficient material to produce visible green emission at 546 nm. Green emission possessed by these glasses is also further confirmed by CIE chromaticity coordinates.